

# Sharp Switching in Optical Couplers With Variable Coupling Coefficient

Truong X. Tran and Xuan N. Nguyen

**Abstract**—We report the switching behavior of a nonlinear optical coupler consisting of two straight waveguides forming a small angle. A very sharp switching can be obtained with these couplers. The switching power can be reduced up to two times compared to conventional couplers. The multiple switching can also happen at two and even more ranges of input powers. Because light switching is based on the optical Kerr effect, ultrafast switching is possible.

**Index Terms**—Directional couplers, nonlinear fiber optics, nonlinear optical devices, optical switches.

## I. INTRODUCTION

**F**IBER couplers, also known as directional couplers are used routinely for a variety of fiber-optical devices that require splitting of an optical field into two physically separated parts (and vice versa). Although most applications of fiber couplers only use their linear characteristics, nonlinear effects have been studied since 1982 [1]–[3]. Several important nonlinear effects have been thoroughly studied in parallel couplers and can lead to all-optical switching among other applications [1], [4], [5]. Conventional couplers consist of two parallel waveguides (or fibers) which are brought together close enough so that their evanescent fields overlap, thus they have a constant coupling coefficient (CCC) along the propagation direction. It is well-known that the switching sharpness in these couplers is not very good and several approaches have been proposed to overcome this drawback. These new approaches are based on three-core couplers [6]–[8], nonlinear junctions [9], [10], or even a switching matrix [11]. In this paper we show that the ideal switching sharpness and the multiple switching can be realized in a coupler consisting of just two straight waveguides forming a small angle  $\theta$  [see Fig. 1(a)], thus having a variable coupling coefficient (VCC). This kind of coupler has been proposed in a recent study [12] with the focus on the optical non-reciprocity and

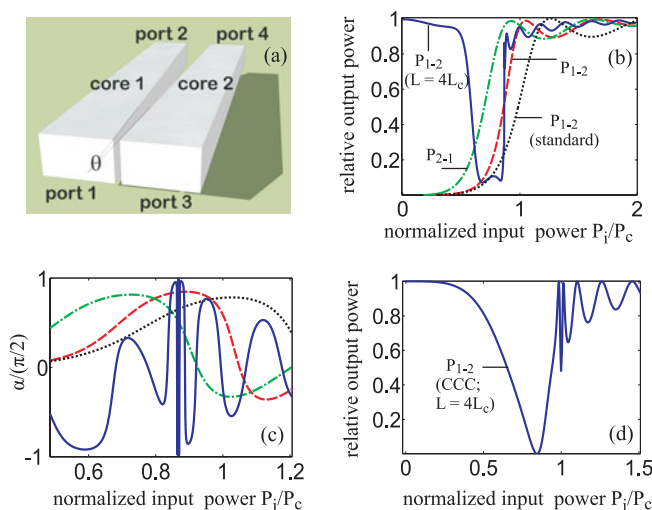


Fig. 1. (Color online) (a) Schematic illustration of a waveguide coupler with two cores forming a non-zero angle  $\theta$ . (b) Relative output power as a function of normalized input power ( $P_i/P_c$ ) in the CW regime. Black dotted curve: the standard switching for couplers having CCC with the length  $L = L_c$ ; red dashed and green dashed-dotted curves: light is launched from port 1, then collected at port 2 and vice versa, respectively, for couplers having VCC with the length  $L = 1.3L_c$ ; blue solid curve: light is launched from port 1, then collected at port 2 for couplers having VCC with the length  $L = 4L_c$ . (c) Normalized angles of the tangent line at each point on the curves in Fig. 1(b) are shown correspondingly in Fig. 1(c). The type and color of curves in Fig. 1(b) and corresponding curves in Fig. 1(c) are the same. (d) Relative output power as a function of normalized input power ( $P_i/P_c$ ) in the CW regime for couplers having CCC with the length  $L = 4L_c$ .

“optical diode” action. Even though in the latter study [12] the switching ability of these couplers has also been mentioned, but it has not been investigated in detail, and other important switching features of these couplers such as switching with ideal sharpness, multiple switching and other aspects have not been reported there. In this paper we intend to explore these important switching features which have been missed in the latter study [12].

The paper is organized as follows. In Section II, we describe the two coupled-mode equations governing the light propagation in couplers consisting of two straight waveguides forming a small angle. In Section III, we investigate the switching behavior in the continuous wave (CW) regime of these couplers. The switching behavior with super-Gaussian pulses is explored in Section IV. In Section V, we summarize our results and finish with concluding remarks.

Manuscript received January 13, 2014; revised February 11, 2014; accepted February 20, 2014. Date of publication February 23, 2014; date of current version March 17, 2014. This work was supported by the German Max Planck Society for the Advancement of Science through the program for Max Planck Partner Groups.

Tr. X. Tran was with the Max Planck Institute for the Science of Light, Erlangen, Germany. He is now with the Le Quy Don University, 10000 Hanoi, Vietnam (e-mail: truong.tran@mpl.mpg.de).

X. N. Nguyen is with the Le Quy Don University, 10000 Hanoi, Vietnam (e-mail: fieldtheory2876@gmail.com).

Color versions of one or more of the figures in this paper are available online at <http://ieeexplore.ieee.org>.

Digital Object Identifier 10.1109/JLT.2014.2307954

## II. THE THEORETICAL MODEL

The two coupled generalized nonlinear Schrödinger equations that describe the system can be written as [4]

$$i\partial_z A_1 + D(i\partial_T)A_1 + \kappa(z)A_2 + \gamma \left(1 + \frac{i}{\omega_0}\partial_T\right) \times A_1(z, T) \int_0^\infty R(t')|A_1(z, T - t')|^2 dt' = 0 \quad (1)$$

$$i\partial_z A_2 + D(i\partial_T)A_2 + \kappa(z)A_1 + \gamma \left(1 + \frac{i}{\omega_0}\partial_T\right) \times A_2(z, T) \int_0^\infty R(t')|A_2(z, T - t')|^2 dt' = 0 \quad (2)$$

where  $A_1$  and  $A_2$  are electric field envelopes in each waveguide,  $z$  is the longitudinal coordinate, and  $T$  is time. The linear dispersion operator and the nonlinear response function are given by  $D(i\partial_T)$  and  $R(t)$ , respectively [see [12] for more details]. The effect of the shock term is through the derivative  $(i/\omega_0)\partial_T$ , where  $\omega_0$  is the central frequency of the input pulse.

In the case of two identical circular cores, the coupling coefficient  $\kappa(z)$  can be calculated by using the following known empirical expression (see [13]):

$$\kappa(z) = \frac{\pi\sqrt{n_{co}^2 - n_{cl}^2}}{2an_{co}} \exp[-(c_0 + c_1\bar{d}(z) + c_2\bar{d}^2(z))] \quad (3)$$

where  $a$  is the cores radius,  $n_{co,cl}$  are the refractive indices of cores and cladding, respectively, and  $\bar{d}(z) \equiv d(z)/a$  is the normalized center-to-center spacing between the two cores ( $\bar{d} > 2$ ). Constants  $c_0$ ,  $c_1$ , and  $c_2$  depend on the fibers  $V$ -parameter (see [12] and [13]). If the angle between the two cores of the coupler equals  $\theta$ , then  $\bar{d}(z)$  varies along  $z$ . As a result, the coupling coefficient  $\kappa(z)$  is not a constant along  $z$ :  $\kappa(z) = \kappa_0 \exp(-\alpha_1 z - \alpha_2 z^2)$ , where  $\kappa_0 \equiv [(\pi\sqrt{n_{co}^2 - n_{cl}^2})/(2an_{co})] \exp(-c_0 - c_1 d(0)/a - c_2 d^2(0)/a^2)$ ,  $\alpha_1 = c_1\theta/a$ , and  $\alpha_2 = c_2\theta^2/a^2$ . This forward-backward asymmetry of the structure leads to the optical non-reciprocity in the light propagation [12]. In the case of square cores, it turns out that one can still use (3) to approximately calculate the coupling coefficient if the effective core radius  $a_{\text{eff}} = b/\sqrt{\pi}$ , where  $b$  is the side of square cores, is used instead of the core radius  $a$  [12]. We now introduce dimensionless variables  $\xi = z/z_0$ ,  $\tau = T/T_0$ ,  $u = A_1/\sqrt{P_0}$  and  $v = A_2/\sqrt{P_0}$ , where  $z_0 = 1/\kappa_0$ . The power scale is  $P_0 = 1/(\gamma z_0)$ . With these new variables, Equations (1)–(2) are equivalent to the following dimensionless equations:

$$i\partial_\xi u + \frac{z_0}{L_D} D(i\partial_\tau)u + v \exp(-\alpha_1 z_0 \xi - \alpha_2 z_0^2 \xi^2) + \left(1 + \frac{i}{\omega_0 T_0} \partial_\tau\right) u \int_0^\infty r(\tau')|u(\xi, \tau - \tau')|^2 d\tau' = 0 \quad (4)$$

$$i\partial_\xi v + \frac{z_0}{L_D} D(i\partial_\tau)v + u \exp(-\alpha_1 z_0 \xi - \alpha_2 z_0^2 \xi^2) + \left(1 + \frac{i}{\omega_0 T_0} \partial_\tau\right) v \int_0^\infty r(\tau')|v(\xi, \tau - \tau')|^2 d\tau' = 0 \quad (5)$$

where  $L_D = T_0^2/|\beta_2|$ ,  $\beta_2$  is the group velocity dispersion, the dimensionless function  $r(\tau)$  is obtained by rescaling time  $t$  with

$T_0$  in the response function  $R(t)$  (see [12]). The standard split-step Fourier method [14] will be adopted for simulations in this paper.

## III. OPTICAL SWITCHING IN THE CW REGIME

In the CW regime, the dispersion terms in (4)–(5) will be eliminated, whereas the nonlinear parts will now contain just the well-known Kerr terms for materials with Kerr nonlinearity. In this paper we investigate the widespread material  $Al_xGa_{1-x}As$  which has a great nonlinearity  $n_2 = 1.5 \times 10^{-13} \text{ cm}^2/\text{W}$  and low loss in the infrared region where the photon energy is less than half the semiconductor bandgap [15]. The refractive index of this material can be calculated and depends on the parameter  $x$  [16]. The coupler is formed by two identical step-index square waveguides with cladding having  $x = 0.185$ , and core having  $x = 0.18$ . The similar (but not exact) compositions have been used to fabricate waveguide arrays [17]. Note that the concepts expressed here are independent of the precise nature and geometry of the two waveguides, provided that they are identical.

Fig. 1(b) shows the relative output power  $P_{i-j}$ , which denotes the ratio of the output power at the port  $j$  to the total input power  $P_i$  launched into the system through the port  $i$ , as a function of the normalized input peak power  $p = P_i/P_c$ , where  $P_c \equiv 4\kappa_0/\gamma = 4P_0$ , see [4]. The black dotted curve represents the well-known standard switching  $P_{1-2}$  for conventional two-core couplers having CCC with the length  $L = L_c = \pi/(2\kappa_0)$  [18]; red dashed and green dashed-dotted curves show the switching when light is launched from port 1, then collected at port 2 and vice versa, respectively, for couplers having VCC with the length  $L = 1.3 L_c$  (these two curves also demonstrate the non-reciprocity in couplers having VCC, see [12]); blue solid curve demonstrates the switching when light is launched from port 1, then collected at port 2 for couplers having VCC with the length  $L = 4 L_c$ . Parameters used to obtain Fig. 1(b) are: effective core radius of the two square cores  $a_{\text{eff}} = 2 \mu\text{m}$ , center-to-center spacing at the front end  $\bar{d}(0) = 4.0$ , angle between two cores  $\theta = 3.4 \text{ mrad}$ , wavelength  $\lambda = 1.55 \mu\text{m}$ . With these parameters the power scale is calculated to be  $P_0 = 660 \text{ W}$ , coupling length  $L_c \simeq 0.49 \text{ mm}$ , and the nonlinear parameter  $\gamma = 4.8 \text{ W}^{-1}/\text{m}$ . Fig. 1(c) plots the normalized angle of incline  $\alpha/(\pi/2)$  of the tangent line at each point on the curves shown in Fig. 1(b). The type and color of curves in Fig. 1(b) and corresponding curves in Fig. 1(c) are the same. The switching sharpness of couplers can be quantitatively characterized by the absolute value of the normalized angle of incline  $|\alpha|/(\pi/2)$ . In terms of switching sharpness, the switching is ideal if the angle of incline of curves shown in Fig. 1(b) would be  $|\alpha| = \pi/2$  in the switching region. In that case, a slight change of the input power will be able to switch the output signal from one output port to the other one. In other words, the greater  $|\alpha|$ , the better the switching sharpness of couplers. From Fig. 1(b) and (c) one can have following remarks.

Firstly, the switching sharpness of couplers having VCC is improved as compared to the standard switching in conventional two-core couplers having CCC, and it can be almost ideal in the case of the coupler length  $L = 4 L_c$  (see solid blue curve with the vertical fragment). Indeed, one can see from

Fig. 1(b) that the slope at the switching region (when the normalized input power is around unity) of the curve representing the conventional two-core couplers having CCC (the black dotted curve labeled “standard”) is less steep than slopes of other curves representing couplers having VCC. This feature is also demonstrated in Fig. 1(c), where the maximum absolute value of the normalized angle of incline of the tangent lines will be  $|\alpha|/(\pi/2) = 0.7863, 0.8176, 0.85,$  and  $0.96,$  respectively, for the black dotted curve representing couplers having CCC, the green dashed-dotted curve representing couplers having VCC with the coupler length  $L = 1.3L_c,$  and the solid blue curve representing couplers having VCC with the coupler length  $L = 4L_c.$  The increase in switching sharpness of couplers having VCC can be explained qualitatively as follows. To be specific, we will now focus on the red dashed curve labeled “ $P_{1-2}$ ” in Fig. 1(b) where light propagates from the front end to the rear end in Fig. 1(a). First, it is well-known that for conventional couplers, in the linear regime when the input power is small, at the coupler length  $L = L_c = \pi/(2\kappa_0),$  light launched at one core will be completely transferred into the other core [4]. This is the case with the black dotted curve labeled “standard” in Fig. 1(b). However, for couplers having VCC, when moving from the front end to the rear end in Fig. 1(a) the coupling coefficient will decrease [ $\kappa(z) < \kappa_0$ ], as a result, the *effective* coupling length for couplers having VCC will now be larger than  $L_c = \pi/(2\kappa_0),$  and for the specific set of parameters used in Fig. 1 the effective coupling length for couplers having VCC equals to  $1.3L_c.$  That is the case of the red dashed curve labeled “ $P_{1-2}$ ” in Fig. 1(b). Second, it is also well-known that for conventional couplers, at the coupling length, the switching happens around the input power  $P_i = P_c = 4\kappa_0/\gamma$  [4] [see the curve labeled “standard” in Fig. 1(b)], however, for couplers having VCC we have  $\kappa(z) < \kappa_0,$  as a result, the switching power for couplers having VCC is smaller than in the case of conventional couplers. Thus, we can interpret that the red dashed curve labeled “ $P_{1-2}$ ” in Fig. 1(b) is formed by shifting the top part of the black dotted curve labeled “standard” in Fig. 1(b) to the left side while fixing the bottom part. This is a possible reason why the switching sharpness is enhanced in couplers having VCC as compared to conventional couplers.

Secondly, as explained previously, from Fig. 1(b) one can easily see that the switching power in couplers having VCC is smaller and can be reduced up to two times compared to the standard switching power. Because the switching sharpness in three-core couplers is improved at the expense of the higher switching power in comparison to the standard switching [6], [7], thus the switching power in couplers having VCC can be even much smaller than the one in three-core couplers.

Thirdly, in the case of couplers having VCC the multiple switching is possible if the coupler is long enough. For instance, when  $L = 4L_c$  as indicated by the blue solid curve with U-like pattern in Fig. 1(b), the switching can happen around two normalized input powers  $P_i/P_c = 0.59$  and  $0.86$  (compared to  $P_i/P_c = 1.07$  for couplers having CCC). This multiple switching has also been reported for nonlinear junctions [9], [10]. It is worth mentioning that in the case of conventional couplers having CCC the coupler length is a crucial parameter determining switching characteristics. It can be numerically shown that the

overall switching characteristics in couplers having CCC will be worse if the coupler length is much different from  $L_c.$  On the contrary, the length of couplers having VCC can be chosen in a much larger range in which they still maintain good performance as switching device.

For the sake of completeness in comparing the switching performance between couplers having CCC and VCC, and also for understanding the reason why the multiple switching is possible with couplers having VCC, in Fig. 1(d) we show the relative output power  $P_{i-j}$  as a function of the normalized input peak power  $p = P_i/P_c$  for conventional two-core couplers having CCC with coupler length  $L = 4L_c.$  It is clearly shown in Fig. 1(d) that the switching performance of couplers having CCC gets worse in this case as compared to couplers having VCC. Indeed, although from the bottom of the letter V one can switch into both sides and vice versa, but because the region of the bottom of the letter V is very tiny (unlike the letter U), it would be difficult to switch exactly into the bottom of the letter V (and we need to switch into that bottom in order to have a good switching contrast). Moreover, the oscillatory features on the right-hand side of the letter V in Fig. 1(d) have big amplitudes, thus they would decrease the switching contrast when the switching takes place from the bottom of the letter V to the right-hand side and vice versa. As clearly shown in Fig. 1(b) and (d), at the length  $L = 4L_c$  another weak point of couplers having CCC is the switching sharpness with the letter V as compared to the letter U. The similar switching behavior with V-like pattern also happens at the coupler length  $L = 2L_c$  for conventional couplers. This is understandable, because for conventional couplers with the length  $L = 2qL_c,$  where  $q$  is an integer number, in the linear regime when the input power is small, at the output light will be transferred back to the input core [4]. Meanwhile, at large input powers, light also gets trapped in the same input core. On the other hand, at the intermediate input powers a big amount of input light can be transferred to the other core. Therefore, the switching with V-like pattern is possible in conventional couplers with the length  $L = 2qL_c.$  For couplers having VCC, the switching with V-like pattern can also be possible, however, as explained above, the switching sharpness of couplers having VCC is enhanced as compared to conventional couplers, thus the letter V is transformed into the U letter. This is a possible mechanism explaining the multiple switching with U-like pattern in couplers having VCC as shown in Fig. 1(b). Note that unlike the coupler length  $L = 2qL_c$  with  $q$  being an integer number required to form the V-like pattern for conventional couplers, in order to obtain the U-like pattern for couplers having VCC the coupler length can be varied in a large range, provided that couplers are long enough. The specific coupler length  $L = 4L_c$  with the factor of 4 for the U-like pattern shown in Fig. 1(b) for couplers having VCC is just a coincidence.

One of crucial parameters for couplers having VCC operating as a switching device is the angle  $\theta$  formed by the two cores. It is obvious that the angle cannot be large, otherwise, the coupling coefficient will decrease (increase) extremely fast along  $z$  if light propagates from the front (rear) end to the rear (front) end in Fig. 1(a). As a result, the device will operate as a coupler for a very short length at the front end, but for the big portion at the rear end the two cores are practically not coupled. For

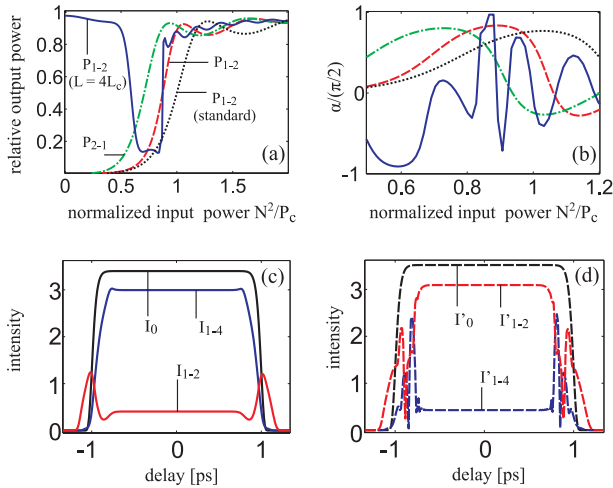


Fig. 2. (Color online) Switching for super-Gaussian input pulse with  $m = 15$  in couplers having VCC. All labels in Fig. 2(a) have the same meanings as labels in Fig. 1(b). (b) Normalized angles of incline of the tangent line at each point on the curves in Fig. 2(a) are shown correspondingly in Fig. 2(b). The type and color of curves in Fig. 2(a) and corresponding curves in Fig. 2(b) are the same. (c) and (d) Intensity profiles for the input and output pulses when  $p = N^2/P_c = 0.85$  and 0.88, respectively, for couplers having VCC with length  $L = 4L_c$ .

such a short coupler length the device is not able to perform the switching well. On the other hand, if the angle  $\theta$  is too small, we will have a device similar to conventional couplers. For specific parameters used in Fig. 1 our simulations show that, in order to perform the switching well, the angle  $\theta$  should have a value of several milliradian.

#### IV. OPTICAL SWITCHING WITH PULSES

High power CW beams often cause damage to optical materials. A common practical solution is to use pulses with high peak power. When input pulses are used instead of CW beams, one needs to use all terms in (1)–(2) and in (4)–(5). It has been experimentally demonstrated that in conventional two-core couplers square pulses can be switched much better than bell-shaped pulses [18]. So, in this paper we will focus on super-Gaussian pulses with flat top which resemble square pulses. Fig. 2(a) illustrates this case when a super-Gaussian pulse is launched at one port, for instance  $A_1 = N \exp[-0.5(t/T_0)^{2m}]$  and  $A_2 = 0$  with  $T_0 = 1$  ps and  $m = 15$ . The super-Gaussian pulse will resemble the square pulse more and more when the parameter  $m$  increases. All curves shown in Fig. 2(a) denote the same meanings as the corresponding ones in Fig. 1(b) (only now the input is a super-Gaussian pulse). The normalized angle of incline  $\alpha/(\pi/2)$  of the tangent line at each point on the curves in Fig. 2(a) are shown correspondingly in Fig. 2(b). The type and color of curves in Fig. 2(a) and corresponding curves in Fig. 2(b) are the same. Comparing Fig. 1(b) with Fig. 2(a), Fig. 1(c) with Fig. 2(b) one can see that switching characteristics such as switching sharpness, switching power, multiple switching with long enough couplers almost remain unchanged, only the switching ratio is slightly reduced in the super-Gaussian case [curves with label  $P_{1-2}$  and  $P_{2-1}$  do not go up to the maximum value (unity) in Fig. 2(a), whereas they do touch that level in Fig. 1(b)]. In most cases, the switching ratio of couplers having VCC and

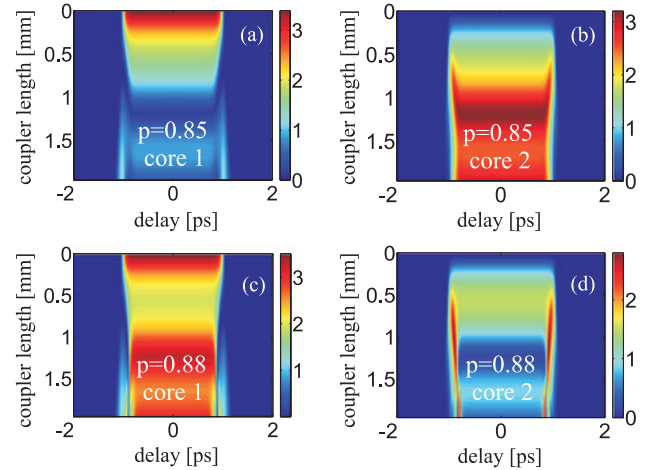


Fig. 3. (Color online) Pulse propagation in cores of couplers having VCC with length  $L = 4L_c$ . (a) and (b)  $p = 0.85$ : pulse is launched from port 1, then propagates in both cores 1 and 2, respectively. (c) and (d) Same as (a) and (b), but now  $p = 0.88$ .

standard ones is practically the same [compare the red dashed and green dashed-dotted curves versus black dotted curves in Fig. 1(b) and Fig. 2(a)]. The switching ratio of couplers having VCC decreases for the case where the multiple switching happens [compare blue solid curves versus other curves in Fig. 1(b) and Fig. 2(a)]. But it is noteworthy to mention that the multiple switching is impossible with standard couplers.

For this specific case with large pulse duration ( $T_0 = 1$  ps) our numerous calculations show that the Raman part contained in the response function  $R(t)$  in (1)–(2) does not play a big role in the pulse propagation process, thus one can simply take the Kerr nonlinearity to simulate (1)–(2).

In the remainder of this paper we will analyze in detail the switching process of that super-Gaussian pulse in couplers having VCC with the length  $L = 4L_c$ . Fig. 2(c) and (d) show the intensity profiles for the input and output pulses when  $p = N^2/P_c = 0.85$  and 0.88, respectively, for couplers having VCC with length  $L = 4L_c$ ; whereas Fig. 3 shows the pulse propagation in two cores of couplers. At first, we take the value  $p = N^2/P_c = 0.85$  for the input pulse [see Fig. 2(c)]. This value corresponds to the input super-Gaussian pulse (launched to the port 1) with the label  $I_0$  in Fig. 2(c) and one point in the dip ( $P_{1-2} = 0.17$ ) of the blue solid curve in Fig. 2(a) close to the vertical fragment. With this initial condition, at the output, only a small portion of energy (17% of the input) will be collected at the port 2 [indicated by the curve with label  $I_{1-2}$  in Fig. 2(c)], whereas much of the energy (83%) will be transferred to the port 4 [indicated by the curve with label  $I_{1-4}$  in Fig. 2(c)]. The pulse propagation in cores 1 and 2 for this case ( $p = 0.85$ ) is shown in Fig. 3(a) and (b), respectively. From Fig. 3(a) and (b) one can see that only a small portion of input energy will remain in the core 1 during the propagation, whereas much of input energy will be transferred from the core 1 to the core 2.

Now the opposite outcome will happen if we slightly increase the energy of the input pulse  $p$  from 0.85 to 0.88 [see the input curve with the label  $I'_0$  in Fig. 2(d)]. With this slight increase in energy for the input, the corresponding point on the blue

solid curve in Fig. 2(a) will jump up from the dip ( $P_{1-2} = 0.17$ ) to the high level ( $P_{1-2} = 0.82$ ). Correspondingly, at the output, a great portion of energy (82% of the input) will now be collected at the port 2 [indicated by the curve with label  $I'_{1-2}$  in Fig. 2(d)], whereas only a small portion of the energy (18%) will be transferred to the port 4 [indicated by the curve with label  $I'_{1-4}$  in Fig. 2(d)]. The pulse propagation in cores 1 and 2 for this case ( $p = 0.88$ ) is shown in Fig. 3(c) and (d), respectively. From Fig. 3(c) and (d) one can see that now a great portion of input energy will remain in the core 1 during the propagation, whereas only a small amount of input energy will be transferred from the core 1 to the core 2. So, it is possible that one can steer a great amount of the energy of a strong input pulse to a desirable output port just simply by turning ON/OFF a very weak controlling pulse. It is noteworthy to mention that the switching in couplers is based on the optical Kerr effect, so the switching could be as fast as 8ps for couplers made of  $Al_xGa_{1-x}As$  [19] and even faster if other materials with almost instantaneous response time for Kerr effect, for instance, fused silica [14], are used.

## V. SUMMARY

In conclusion, we demonstrate numerically that a coupler consisting of two waveguides forming a small angle is able to switch CW beams or super-Gaussian pulses to desirable output ports. The switching characteristics such as switching sharpness, switching power of this coupler are much enhanced as compared to the conventional coupler consisting of two parallel cores. In particular, the switching sharpness of the new couplers can be almost ideal. The switching power of the new coupler is smaller and can be reduced up to two times compared to the standard switching power in the conventional coupler. The multiple switching of the new coupler can also be realized at two and even more ranges of input powers, provided that the coupler length is long enough. Our results suggest that this new kind of coupler can have great potential in ultrafast nonlinear switching applications.

## ACKNOWLEDGMENT

The authors would like to thank F. Biancalana for useful discussions

## REFERENCES

- [1] S. M. Jensen, "The nonlinear coherent coupler," *IEEE J. Quantum. Electron.*, vol. QE-18, no. 10, pp. 1580–1583, Oct. 1982.
- [2] A. A. Maier, "Optical transistors and bistable devices utilizing nonlinear transmission of light in systems with unidirectional coupled waves," *Sov. J. Quantum. Electron.*, vol. 12, pp. 1490–1494, Oct. 1982.
- [3] K. Kitayama and S. Wang, "Optical-pulse compression by nonlinear coupling," *Appl. Phys. Lett.*, vol. 43, pp. 17–19, Apr. 1983.
- [4] G. P. Agrawal, *Applications of Nonlinear Fiber Optics*, 2nd ed. San Diego, CA, USA: Academic, 2008, pp. 54–99.
- [5] S. R. Friberg, A. M. Weiner, Y. Silberberg, B. G. Sfez, and P. S. Smith, "Femtosecond switching in a dual-core-fiber nonlinear coupler," *Opt. Lett.*, vol. 13, pp. 904–906, Oct. 1988.
- [6] Y. Chen, A. W. Snyder, and D. J. Mitchell, "Ideal optical switching by nonlinear multiple (parasitic) core couplers," *Electron. Lett.*, vol. 26, pp. 77–78, Jan. 1990.

- [7] N. Finlayson and G. I. Stegeman, "Spatial switching, instabilities, and chaos in a three-waveguide nonlinear directional coupler," *Appl. Phys. Lett.*, vol. 56, pp. 2276–2278, Jun. 1990.
- [8] M. G. da Silva, A. F. Teles, and A. S. B. Sombra, "Soliton switching in three-core nonlinear directional fiber couplers," *J. Appl. Phys.*, vol. 84, pp. 1834–1842, Aug. 1998.
- [9] Y. Silberberg and B. G. Sfez, "All-optical phase- and power-controlled switching in nonlinear waveguide junctions," *Opt. Lett.*, vol. 13, pp. 1132–1134, Dec. 1988.
- [10] J. P. Sabini, N. Finlayson, and G. I. Stegeman, "All-optical switching in nonlinear X junctions," *Appl. Phys. Lett.*, vol. 55, pp. 1176–1178, Sep. 1989.
- [11] G. J. Liu, J. Liu, B. M. Liang, Q. Li, and G. L. Jin, "Nonlinear optical switching matrix," *Opt. Lett.*, vol. 28, pp. 1347–1349, Aug. 2003.
- [12] Tr. X. Tran and F. Biancalana, "Nonreciprocal behavior and switching in optical couplers with longitudinally varying coupling coefficient," *Opt. Lett.*, vol. 37, pp. 1772–1774, May 2012.
- [13] R. Tewari and K. Thyagarajan, "Analysis of tunable single-mode fiber directional couplers using simple and accurate relations," *J. Lightw. Technol.*, vol. 4, no. 4, pp. 386–390, Apr. 1986.
- [14] G. P. Agrawal, *Nonlinear Fiber Optics*, 5th ed. New York, NY, USA: Academic, 2013.
- [15] F. Lederer, G. I. Stegeman, D. N. Christodoulides, G. Assanto, M. Segev, and Y. Silberberg, "Discrete solitons in optics," *Phys. Rep.*, vol. 463, pp. 1–126, Apr. 2008.
- [16] S. Adachi, "GaAs, AlAs, and  $Al_xGa_{1-x}As$ : Material parameters for use in research and device applications," *J. Appl. Phys.*, vol. 58, pp. R1–R29, Apr. 1985.
- [17] P. Millar, J. S. Aitchison, J. U. Kang, G. I. Stegeman, A. Villeneuve, G. T. Kennedy, and W. Sibbett, "Nonlinear waveguide arrays in AlGaAs," *J. Opt. Soc. Amer. B*, vol. 14, pp. 3224–3231, Nov. 1997.
- [18] A. M. Weiner, Y. Silberberg, H. Fouckhardt, D. E. Leaird, M. A. Saifi, M. J. Andrejco, and P. W. Smith, "Use of femtosecond square pulses to avoid pulse break-up in all-optical switching," *IEEE J. Quantum Electron.*, vol. 25, no. 12, pp. 2648–2655, Dec. 1989.
- [19] A. D. Bristow, J.-P. R. Wells, W. H. Fan, A. M. Fox, M. S. Skolnick, D. M. Whittaker, A. Tahraoui, T. F. Krauss, and J. S. Roberts, "Ultrafast nonlinear response of AlGaAs two-dimensional photonic crystal waveguides," *Appl. Phys. Lett.*, vol. 83, pp. 851–853, Jun. 2003.

**Truong X. Tran** was born in Thai Binh city, in 1975. He received the B.S. and M.S. degrees in laser techniques and laser technologies from the Saint Petersburg National Research University of Information Technologies, Mechanics and Optics, Saint Petersburg, Russia, in 2002 and 2004, and the Ph.D. degree in optics from the same university, in 2007. In 2009–2012, he was a Postdoctoral Researcher at the German Max Planck research group "Nonlinear Photonic Nanostructures" at the Max Planck Institute for the Science of Light, Erlangen, Germany. Since 2013, he has been a Lecturer at the Department of Physics, Le Quy Don University in Hanoi, Vietnam. He is the author of about 30 scientific articles in peer-reviewed journals. His research interests include linear and nonlinear fiber optics, optical solitons, waveguide arrays, photonic crystal fibers, simulation of quantum effects with optical platforms, and laser technologies. Dr. Tran has won a project to establish a Max Planck Partner Group in Hanoi from 2013–2016 with a potential two-year extension (up to 2018). This Partner Group has been financially supported by the German Max Planck Society for the Advancement of Science.

**Xuan N. Nguyen** was born in Hanoi city, in 1976. He received the B.S. and M.S. degrees in theoretical physics and mathematical physics from Hanoi National University, Hanoi, Vietnam, in 1999 and 2003, and the Ph.D. degree in quantum field theory from the same university, in 2009. Since 2009, he has been a Lecturer at the Department of Physics, Le Quy Don University, Hanoi, Vietnam. He is the author of about ten scientific articles in peer-reviewed journals. His research interests include high energy physics, gauge field theory, gravity theory, methods of mathematical physics, and nonlinear fiber optics. Dr. Nguyen has been a member in Dr. Tran's Max Planck Partner Group in Hanoi since 2013.